

UC Santa Cruz

UC Santa Cruz Previously Published Works

Title

Cheap gulp foraging of a giga-predator enables efficient exploitation of sparse prey.

Permalink

<https://escholarship.org/uc/item/1476k209>

Journal

Science Advances, 9(25)

Authors

Videsen, Simone

Simon, Malene

Christiansen, Fredrik

et al.

Publication Date

2023-06-23

DOI

10.1126/sciadv.ade3889

Copyright Information

This work is made available under the terms of a Creative Commons Attribution-NonCommercial License, available at <https://creativecommons.org/licenses/by-nc/4.0/>

Peer reviewed

ECOLOGY

Cheap gulp foraging of a giga-predator enables efficient exploitation of sparse prey

Simone K. A. Videsen^{1,2}, Malene Simon², Fredrik Christiansen^{3,4}, Ari Friedlaender⁵, Jeremy Goldbogen⁶, Hans Malte¹, Paolo Segre⁶, Tobias Wang¹, Mark Johnson^{1,3}, Peter T. Madsen^{1*}

The giant rorqual whales are believed to have a massive food turnover driven by a high-intake lunge feeding style aptly described as the world's largest biomechanical action. This high-drag feeding behavior is thought to limit dive times and constrain rorquals to target only the densest prey patches, making them vulnerable to disturbance and habitat change. Using biologging tags to estimate energy expenditure as a function of feeding rates on 23 humpback whales, we show that lunge feeding is energetically cheap. Such inexpensive foraging means that rorquals are flexible in the quality of prey patches they exploit and therefore more resilient to environmental fluctuations and disturbance. As a consequence, the food turnover and hence the ecological role of these marine giants have likely been overestimated.

INTRODUCTION

Rorqual gigantism evolved some 5 Ma ago in response to increased concentrations of small prey driven by the onset of seasonally intensified upwelling regimes in the ocean (1, 2). Central to this radiation of giga-predators was the evolution of a bulk feeding strategy (1) where tens of tons of water are engulfed in a single mouthful and then filtered in baleen to harvest small fish and zooplankton (Fig. 1) (3). Before opening their parachute-like mouths, lunge feeding rorquals must accelerate to 3 to 5 m/s to maximize the engulfed water volume and reduce prey escapes (4, 5). The resulting high kinetic energy is lost as the whale decelerates because of the momentum transferred to the engulfed water as well as the increased drag from the distended body profile (3, 5). The high drag of lunge feeding suggests high foraging costs, and this inference has been used to explain the unusually short dive times of rorquals (6–8). Humpback whales (*Megaptera novaeangliae*), for example, perform foraging dives that are an order of magnitude shorter than the similar-sized sperm whale (*Physeter macrocephalus*) (9). The predicted high cost of lunge feeding also implies that rorquals must selectively target dense, high-quality prey patches. This requires in turn that they are capable of assessing prey patch quality (6), although the sensory modalities to support such assessment remain unknown.

Their extreme body size and apparent reliance on dense prey suggest that rorquals may be highly susceptible to feeding disruptions due to climate change, anthropogenic noise, and competition with fisheries (10, 11). Extrapolating the presumed large food turnover of rorquals to prewhaling population levels also leads to the conclusion that they exert substantial top-down control on high-latitude marine food chains (11, 12), thereby contributing to global

carbon turnover (13). Such cosmopolitan giga-predators may even act as ecosystem engineers, effectively farming prey by nutrient cycling (11, 14). However, these profound ecological top-down effects involve the presumption that lunge feeding in giant rorquals is energetically costly, a hypothesis that has not been field-tested. Here, we address that hypothesis by measuring the absolute energetic costs of lunge feeding in humpback whales. As capital breeders, humpback whales must meet their annual energetic requirement during a short foraging period in nutrient-rich, high-latitude foraging grounds (12, 15). We used high-resolution biologging tags to record lunge feeding and breathing rates as a proxy for energy expenditure of humpback whales in two polar feeding areas.

RESULTS AND DISCUSSION

We analyzed 338 hours of high-resolution biologging data from 23 whales containing 6633 lunges and 23,416 breaths (table S1). The energetic cost of lunge feeding was quantified from the relationship between feeding and breathing rates in 1-hour intervals (fig. S12). Compared to whales on the breeding grounds (15), we found that whales on the feeding grounds had elevated breathing rates even when not lunging (generalized linear mixed effects model (GLMM) intercept on feeding ground: 61.2 ± 3.3 breaths hour⁻¹ versus breeding ground: 42 ± 12 breaths hour⁻¹ (15); Fig. 2 and fig. S8). However, when feeding, there was only a small increase in breathing rate (mean = 0.58 breath/lunge, Fig. 2) as lunge rate increased for humpback whales in both feeding areas (Fig. 2).

Using a Monte Carlo modeling approach based on estimated distributions of lung tidal volumes and oxygen uptakes (Fig. 3 and fig. S7), we converted breath counts into estimates of energy turnover. We find that the median estimated costs of an average lunge is just 0.77 MJ for a 30-t humpback whale. Even when using the 95% percentile of estimated energy turnover per breath to account for potentially heavier breathing after exercise (16), we find that an average lunge has a maximum metabolic cost of 1 MJ (Fig. 3J). If all of this energy is invested in muscle action during the active part of the lunge, a 30-t humpback whale performs maximum

Copyright © 2023 The Authors, some rights reserved; exclusive licensee American Association for the Advancement of Science. No claim to original U.S. Government Works. Distributed under a Creative Commons Attribution NonCommercial License 4.0 (CC BY-NC).

¹Zoophysiology, Department of Biology, Aarhus University, Denmark. ²Greenland Climate Research Centre, Greenland Institute of Natural Resources, Nuuk, Greenland. ³Aarhus Institute of Advanced Studies, Aarhus University, DK-8000 Aarhus C, Denmark. ⁴Marine Mammal Research, Department of Ecoscience, Aarhus University, 4000 Roskilde, Denmark. ⁵Institute of Marine Sciences, University of California, Santa Cruz, Santa Cruz, CA, USA. ⁶Hopkins Marine Station, Department of Biology, Stanford University, Pacific Grove, CA, USA.

*Corresponding author. Email: peter.madsen@bio.au.dk

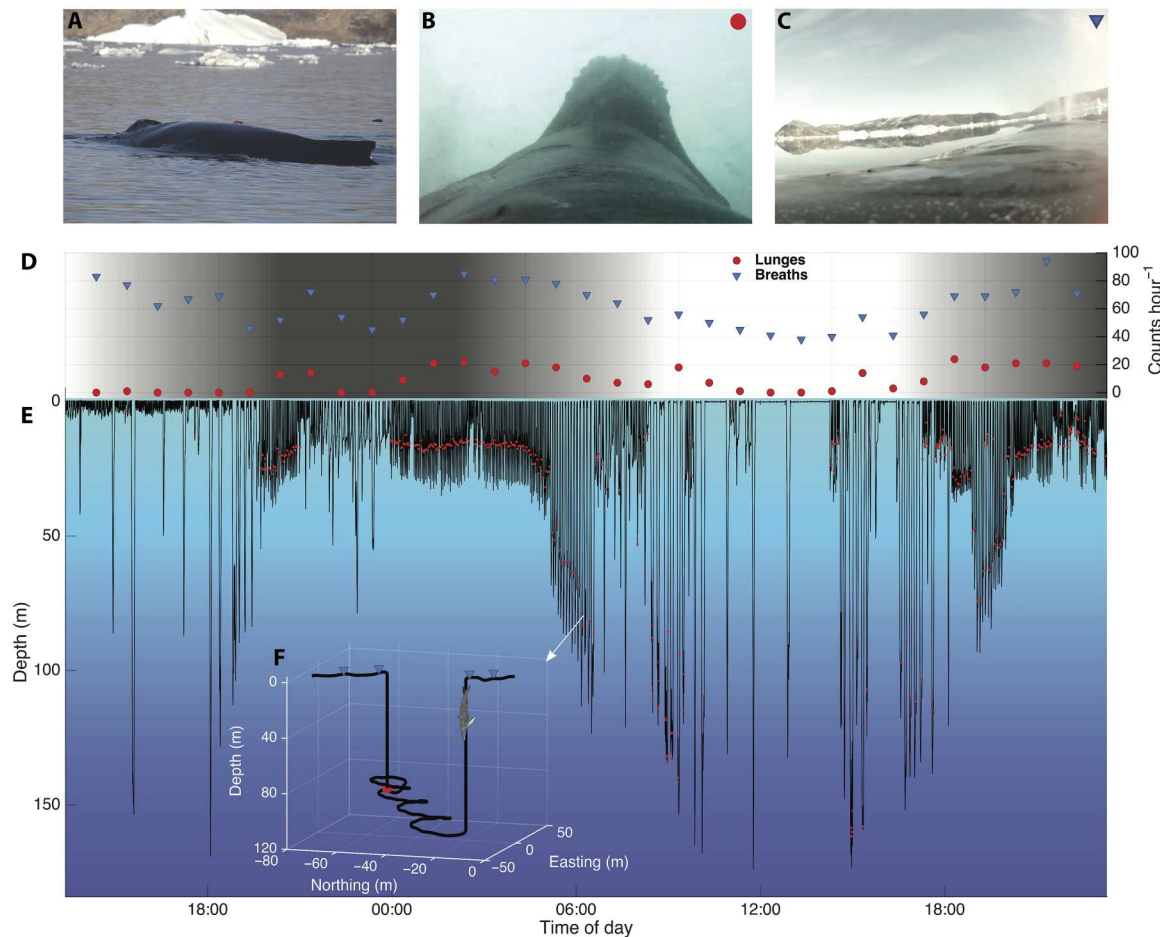


Fig. 1. Diving behavior of a feeding humpback whale. (A) Tagged whale (red tag). (B) Video still frame of lunge feeding humpback whale seen from tag view. (C) Video still frame of tag view of a breath. (D) Hourly breaths (blue triangles) and lunges (red circles) of a tagged whale (mn17_251a). Background shading indicates light level. (E) Dive profile of the same whale with detected lunges (red circles). (F) 3D plot of a feeding dive with lunge (red circle) and breaths (blue triangles) plotted.

mechanical work of no more than 8.3 J/kg of body mass per lunge (Eq. 8), assuming a muscle efficiency of 25% (17). This is comparable to the mass-specific mechanical work done by a terrestrial animal climbing 87 cm vertically, for example, a human walking up three steps of stairs. As the active part of a lunge lasts 5 to 10 s (4, 5), the mean power output is around 1 Watt/kg (equivalent to a jogging human) when a lunging whale is fluking to gain speed before mouth opening (18). Despite the high speeds and massive water engulfment of lunges, this moderate power output combined with the short active duration of lunges results in low mass-specific energy costs. Consequently, the very short dives of rorquals cannot be explained by the energetic expense of lunge feeding (7) but instead may be a result of proximate epipelagic food that places little selection pressure on high-oxygen stores and prolonged dive times (9).

Converting the median metabolic cost of a lunge of 0.77 MJ into absolute prey mass gives a break-even cost of 225 g of prey using an average value of 3800 kJ kg⁻¹ wet weight (ww) (9, 11) and a digestive efficiency of 90% (19). Thus a 30-t humpback whale expends net zero energy in a lunge that yields merely 225 g of prey in the approximately 21 m³ of engulfed water (11), equivalent to one capelin m⁻³ or about 10 krill m⁻³. Despite the persistent narrative that lunges are

highly energetic (4, 6–8, 20), our median lunge cost estimate of 0.77 MJ is within the range of estimates from biomechanical models that report costs between 0.5 and 2.6 MJ per lunge (6, 18, 20–22). Thus, both our field respirometry estimates and biomechanical modeling of acceleration and speed data from biologging show that foraging costs are low in humpback whales despite a high-drag feeding mechanism. Low foraging costs and high engulfment capacity in rorquals mean that these giant predators can feed efficiently on relatively sparse prey. This frees humpback whales from their assumed strict reliance on dense, high-quality prey patches and helps explain the diversity of foraging styles and prey types exploited by this species (5). Given the low break-even ingestion, humpback whales can perhaps even use lunging as a patch assessment tool, obviating the need for sophisticated sensory means to assess prey patch quality.

However, low-cost foraging does not free humpback whales from a time crunch caused by their migratory lifestyle. Humpback whales perform annual long-distance migrations between productive high-latitude feeding grounds and warmer sheltered waters where successful mating and breeding depend on good body condition (23). Because humpback whales scarcely feed on the breeding grounds, the energy spent there is fueled by energy reserves

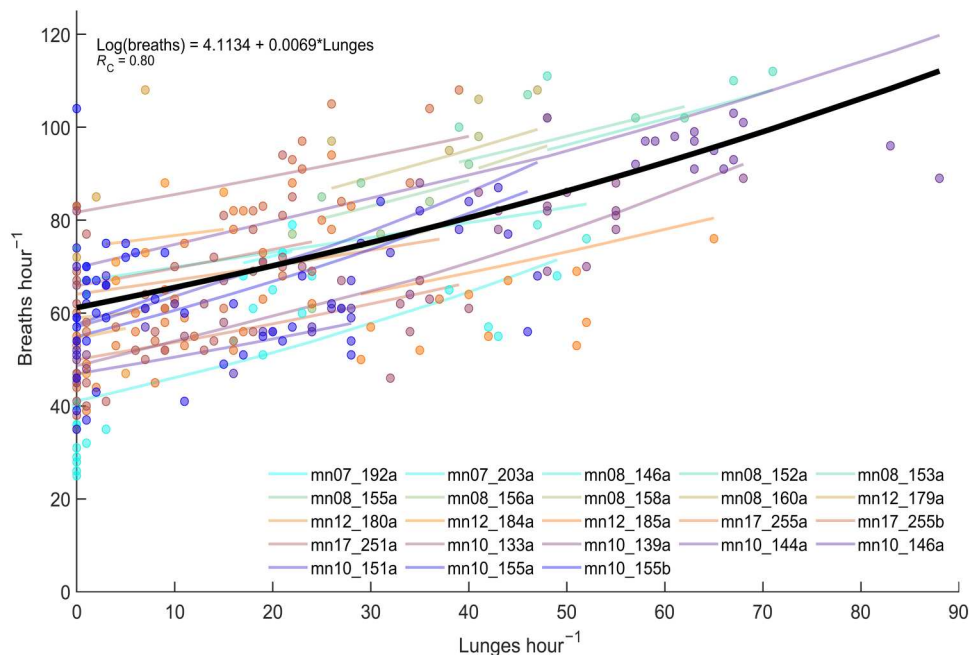


Fig. 2. The relationship between lunges and breaths. Each circle represents counts of breaths and lunges per hour for each whale (colors). Colored lines represent regression lines for individual whales (random effects) and the main model (black line). Marginal $R^2 = 0.29$ (i.e., proportion of total variance explained by fixed effects); conditional $R^2 = 0.80$ (i.e., the contribution of fixed and random effects to total variance).

primarily in the form of blubber generated while on the feeding grounds (23). As a result, humpback whales must largely feed for the year in just 3 to 4 months (11, 24). Using breathing rates of humpback whales from both feeding and breeding grounds (fig. S8), we estimate the annual energy budget of a 30-t whale to be around 700 GJ. Converting this to prey intake and adding costs for somatic growth (5%), we estimate a consumption of 197 ± 47 t/year for a 30-t nonbreeding whale (Fig. 3G). Allowing an additional 10% food intake per year to pay for gestation and lactation every 2 years yields an estimate of 216 ± 52 t/year for a 30-t reproducing female. These numbers imply that a 30-t whale consumes ~6 to 7 times its own body mass each year. In comparison, a recent study of peak prey patch densities around feeding rorquals suggested that a 30-t humpback whale eats 13 to 40 times its own body weight annually (fig. S11; 16). Such high intake estimates imply that humpback whales are hypermetabolic, whereas our estimate of yearly food requirements puts humpback whales below scaling predictions for marine mammal predators (25) and on par with predictions from the standard mouse-to-elephant curve for field metabolic rates (FMRs) (fig. S11). We therefore conclude that humpback whales, and perhaps other rorquals, are not as expensive as suggested by extrapolating the food intake of whales foraging in dense prey fields (11). Thus humpback whales exert some top-down control over high-latitude marine food webs, particularly in prewhaling ecosystems, but perhaps no more so than other marine endotherms such as the smaller, but much more abundant sea birds and pinnipeds that have high mass-specific metabolic rates.

Despite the low cost of lunge feeding, we find that humpback whales expend about two times more energy when on the feeding grounds as compared to the breeding grounds. To explain this, we evaluated the separate costs of ingestion and digestion. We estimate that an adult humpback whale performs some $60,000 \pm 15,000$

lunges per year (Fig. 3I), which, in combination with an annual food requirement of 216 t, implies that reproducing humpback whales on average must ingest 3.8 ± 2 kg of prey per lunge (Fig. 3J), suggesting an average foraging efficiency ratio of about 15 (3800 g/225 g). As for all predators, some 12% of the nutritional value of these protein and fat-filled prey is needed to pay for digestion (26). Therefore, the average energetic cost of digesting the food obtained in one lunge will be about twice the average direct biomechanical costs of the lunge (12% of 3.8 kg = 456 g of prey to pay for digestion versus 225 g of prey to pay for a lunge). If essentially all digestion takes place during only 3 to 4 months on the feeding grounds, FMRs in those months will be elevated by about 50% because of the digestive costs alone compared to the months on breeding grounds where little to no digestion takes place. Thus, as for large reptiles with protracted periods of fasting and intense periods of foraging, much of the elevated FMR observed on the feeding grounds compared to breeding grounds in large capital breeding rorquals [figs. S8 to S9; (15)] is likely not driven by expensive lunge feeding but may be explained by more active swimming to find food and, importantly, the high specific dynamic action required to digest a year's worth of food in just 3 to 4 months.

Our estimated average intake of 3.8 kg/lunge allows for a reevaluation of the prey patch densities required to support feeding humpback whales (11). The engulfment capacity of humpback whales is 15 to 27 m^3 with a mean of 21 m^3 per lunge (11, 27). Assuming a 50% catch rate of prey (22), an average prey density of 0.37 kg m^{-3} is needed to obtain an average of 3.8 kg of prey per lunge, which is within the observed krill and fish densities in feeding areas (11, 21, 28, 29). Remarkable footage of feeding humpback whales show that they sometimes engulf particularly dense prey patches [movie S4; (22, 29)] to achieve extraordinarily high foraging efficiencies. In these extreme cases, peak densities from echo sounder

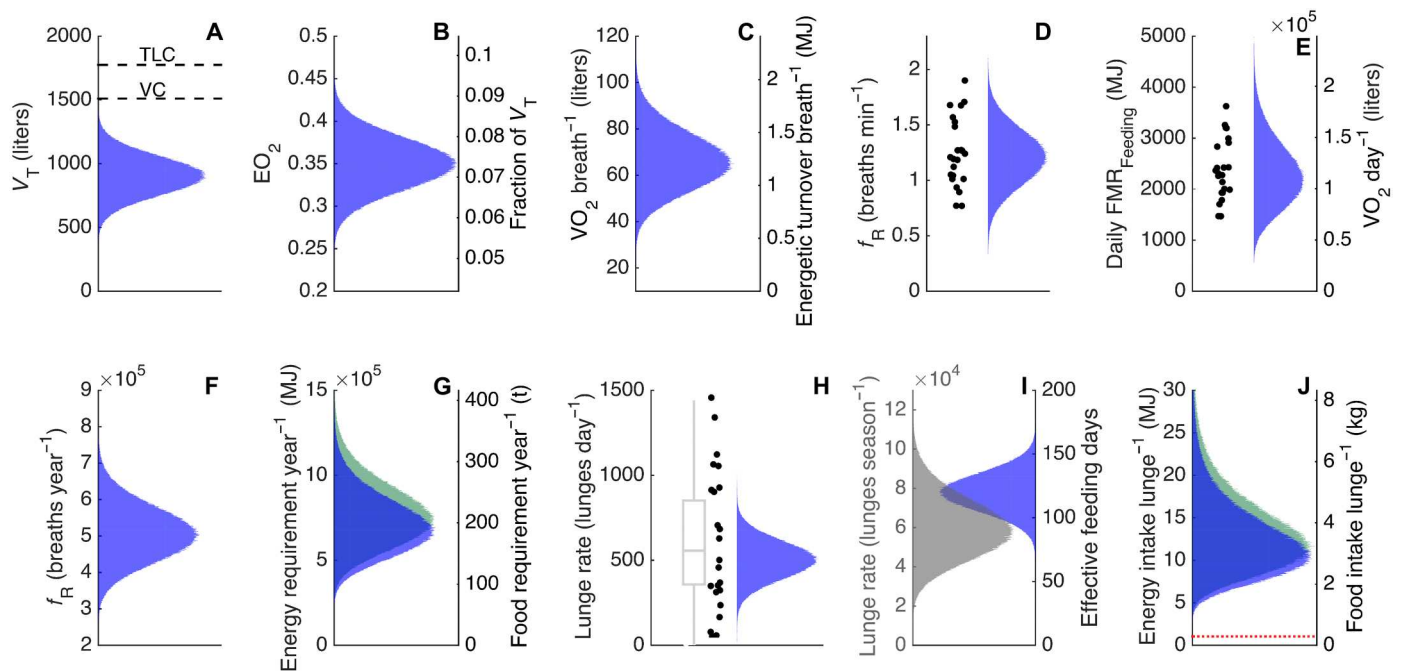


Fig. 3. Modeled food consumption of humpback whales. Estimating consumption from breathing rate involves several parameters that are not precisely known for humpback whales. Each plot indicates the probable distribution of a parameter based on measurements (black dots) and information in the literature. All plots assume a body mass of 30 t. (A) Tidal volume with total lung capacity (TLC) and vital capacity (VC) displayed as black lines. (B) Oxygen extraction coefficient (EO_2). (C) The VO_2 per breath and energetic turnover per breath (MJ). (D) Breathing rate (breaths min^{-1}) (f_R). Black dots represent breathing rates from current study. (E) Daily field metabolic rate (FMR) of feeding humpback whales. Black dots represent calculated daily FMR for each feeding whale in current study. (F) Simulated total breath count during a year, based on breathing rates on feeding and breeding grounds and simulated breathing rates for migrating whales (fig. S8). (G) Annual energy expenditure for a pregnant female humpback whale (green) and nonpregnant adult (blue) based on the total yearly breath count (MJ). (H) Daily lunge rate. Black dots represent data from current study, and gray boxplot represents modeled feeding rates of humpback whales from a previous study (11). (I) Effective feeding days, the days spent feeding while on the feeding grounds and yearly lunge rate. (J) Required energy intake per lunge to cover annual energy expenditure during feeding, migration, and breeding periods for a pregnant female humpback whale (green) and nonpregnant adult (blue). The red line represent the break-even cost of a lunge.

surveys (11, 21, 22, 29) suggest that humpback whales may ingest tens of kilograms of prey per lunge, but our estimated average intake show that such very successful lunges are rare (movies S1 to S3). Instead, food returns per lunge are likely to be log-normally distributed (29) over a season with fewer rich patches interspersed with many more poor ones. Thus, low-cost foraging in humpback whales, and likely other rorquals such as fin and blue whales (fig. S10), enables much greater flexibility in foraging behavior than recent studies suggest (10). Rather than lunge feeding representing an evolutionary cul de sac restricting rorqual baleen whales to target only the densest prey patches, cheap lunge feeding is a very efficient harvesting strategy that allow these giga-predators to exploit a wide density range of tiny prey species on their high-latitude feeding grounds during short foraging seasons. Such flexibility may make humpback whales less vulnerable to variability in prey patch density due to environmental change or human disturbance (10), perhaps explaining the rapid recovery of many subpopulations from whaling (30, 31).

MATERIALS AND METHODS

Tag data

Between 2007 and 2017 16 adult (>10 m) humpback whales were tagged with digital animal-borne loggers in three locations in Greenland: Nuuk fjord, Disko Bay, and fjords around Tasiilaq

(table S1). The research in Greenland was carried out under permits issued by The Ministry of Fishing, Hunting and Agriculture, Greenland Self Government to the Greenland Institute of Natural Resources, according to §35 of the executive order no. 12 of 22 December 2014. In addition, seven adult humpback whales were tagged in 2010 in Wilhelmina Bay, on the Western Antarctic Peninsula (table S1). The research in Antarctica was conducted under National Marine Fisheries Service Permit 808-1735, Antarctic Conservation Act Permit 2009-014, and Duke University Institutional Animal Care and Use Committee A049-112-02. The whales were all equipped with noninvasive suction cup tags, either Dtag version 2 or 3 or CATS tags (Customized Animal Tracking Solutions; www.cats.is/cats-cam/). Both tag types recorded continuous high-resolution sensor data from the whale including pressure and accelerometer data (sampling rate Dtag: 50 Hz, 200 Hz; sampling rate CATS tag: 400 Hz). The Dtag also recorded continuous stereo sound (sampling rates: 48, 64, 96, or 120 kHz, 16 bit) from two hydrophones and the CATS tag recorded video from a forward-pointing video camera (1280 × 720p high-definition resolution) during periods with sufficient light. All whales were tagged from a small motorized vessel that approached slowly from behind (4, 32). To minimize effects of behavioral reactions to tagging in the data analysis, the first hour of tag data was excluded from all analyses sensu (10). Tag attachment durations varied between 3.5 and 34.9 hours (table S1). All Dtags were deployed with a preset galvanic

release, but the suction cup–attached tags sometimes came off prematurely because of rubbing, breaching, or high-intensity swimming.

Detection of lunges

The short burst of fluking during lunge feeding can be detected by sudden changes in the acceleration recorded by animal-attached tags (4, 8) (fig. S1). An automated detector was used to identify jerk peaks [i.e., transients in the differential of acceleration; see methodology in (33)] in the tag recordings. As other high-intensity activities such as excessive fluking (34), breaching (15, 18), and rubbing also give rise to an increase in jerk signal, every detected jerk peak was inspected for stereotyped changes in pitch and roll sensu (4, 5). Furthermore, foraging lunges were verified if a jerk peak was associated with an increase and rapid decrease in flow noise as the whale accelerates forward and then decelerates (fig. S1) (4). This was checked in all Dtag data by listening to, and inspecting spectrograms of, the corresponding sound recording.

Deployments with CATS tags did not record any sound; therefore, when available, video recordings were used to verify jerk-detected lunges. Video cues for lunges included a visible mouth opening with a simultaneous jerk peak (movies S1 to S4). When video was not available, lunge events were inferred from jerk peaks and changes in pitch and roll (4, 5, 35). For each whale, the tag data were divided into 60-min bins, and for each time bin, the number of lunge events were identified.

Detection of breaths

Field and video observations of humpback whales show that they generally breathe every time they surface. Breathes were therefore identified by first detecting every time the whale surfaced (36, 37). The rapid air flow and muscle movements when whales breathe create a jerk transient (i.e., pulse in the differential of acceleration; for example, see movies S5 and S6) that can be detected in the accelerometer data collected by the tags, and this was used to validate breath detections derived from surfacing times. To verify each breath and identify breaths during periods of logging and surface behavior, a 60-s interval of the dive profile with superimposed accelerometer data and jerk together with a spectrogram of the sound was visually and aurally inspected for all Dtag data (15, 36). In case of multiple animals breathing simultaneously, only breath sounds with an associated jerk peak were marked as breaths of the tagged whale (for examples, see figs. S2 to S4, audio S1 to S3, and movies S5 and S6) (8, 15). If breath sounds were masked by high-intensity splashes when surfacing, the whale was presumed to respire if roll and pitch values corresponded to an upright whale (37). Breathing sounds were especially difficult to detect during periods of logging and surface traveling in rough seas because of splash sounds on the tag, which also influenced the jerk signal. These periods of uncertainty were therefore excluded from the analysis, amounting to less than 7% of the data. Only complete continuous 1-hour segments for each animal were analyzed (table S1). Breathes from the three whales tagged with CATS tags were marked in the same way as for the Dtag data. Because no audio was available, marked breaths were validated using video, where either a blow or opening of nostrils were visible (movies S5 and S6). Breathing rates for all whales in the study had an overall median of 1.2 ± 0.31 breaths min^{-1} , which matches well with previously reported breathing rates of 1.15 ± 0.97 breaths min^{-1} for

humpback whales on feeding grounds based on 603.3 hours of visual observations (38).

Model selection and validation

Because both the numbers of breaths and lunges per hour are count data, a GLMM with a Poisson error distribution and log link function was developed to investigate the relationship between number of lunges (explanatory variable) and number of breaths (response variable) in hourly time segments. The GLMM was developed in R v.4.0.3 using the `glmmPQL` function (39) in the `Mass` package (40). To account for repeated measurements from the same individuals, whale ID was included as a random effect on both the intercept and slope parameters. Model validation tests were performed to ensure that all model assumptions were met. To investigate homogeneity of variance, scatter plots of residuals versus fitted values and residuals versus explanatory variables were visually examined. Normality of residuals was investigated in histograms of residuals. Overdispersion was tested by dividing the residual deviance with the residual degrees of freedom, with a ratio value (dispersion parameter, ϕ) above 1 indicating overdispersion (the mean of the variance is larger than the mean). There was no sign of overdispersion in our model ($\phi = 0.82$). The data were visually inspected for temporal autocorrelation (nonindependence between data points), using autocorrelation function (ACF) plots, and we found that model residuals were correlated with a lag of 1. To account for this, an AR1 temporal autocorrelation structure with lag 1 was included in the model (fig. S5). The data were also checked for zero inflation by comparing residuals of data subsets with no lunges against data subsets with one or more lunges (fig. S6). Both the conditional (variance explained by the fixed and random effects) and marginal (variance explained by fixed effects only) R^2 were calculated for the model. The marginal R^2 for the model explained 29% of the variance in the data, whereas the conditional R^2 for the model explained 80% of the variance in the data.

Estimation of energetic turnover per breath

The oxygen uptake per breath ($\text{VO}_{2\text{breath}}$) is given by the volume of air exchanged in one breath (the so-called tidal volume, V_T) and the fraction of the oxygen in the inhaled air the whale takes up (the extraction coefficient, EO_2)

$$\text{VO}_{2\text{breath}} = V_T \cdot \text{EO}_2 \cdot F_{\text{I}\text{O}_2} \quad (1)$$

where $F_{\text{I}\text{O}_2}$ is the fraction of oxygen in atmospheric air of 0.2095. These parameters, or their combination, are readily measured in standard respirometry setups with smaller trained marine mammals using, for example, flow-through respirometry (41) or a pneumotachometer and a fast gas analyzer (42, 43). However, while these methods have been used on young gray whale calves (*Eschrichtius robustus*) in captivity (44, 45), they are logistically impossible to use on large whales at sea. Accordingly, researchers have pursued means to use Eq. 1 to estimate $\text{VO}_{2\text{breath}}$ in large, wild cetaceans by making assumptions about the values of V_T and EO_2 for known or estimated body masses. First used by Krogh (46) and later by others (47–50), this modeling approach often involves the assumption that V_T is a high, fixed value of the total lung capacity (TLC). This notion is based on early observations from restrained and hence perhaps stressed marine mammals (51) that reported V_T values very close to the vital capacity (VC, the maximum possible

tidal volume). Most modeling approaches also assume a high fixed EO_2 of around 50% (47–50) again based on observations of restrained cetaceans that have reported consistently high oxygen uptakes in breaths right after prolonged apnea (44). While a recent study show that this approach of assuming fixed V_T and EO_2 can be unexpectedly accurate in estimating the FMR of harbor porpoises (*Phocoena phocoena*) (52), it has attracted criticism for being overly simplistic (16) on the basis of observations from free-moving, trained marine mammals showing that both V_T and EO_2 are lower and more dynamic than often assumed (53, 54). Thus, because V_T and EO_2 are related to the level of exercise (42) and where the breath is made in the dive cycle (16, 53), it is inherently difficult to reliably estimate the oxygen turnover for any particular breath made by a wild cetacean (16). Nevertheless, because any animal on average must be in physiological steady state, the method of estimating VO_2 from the parameters of Eq. 1 lend themselves to quantification of the probability density function of energy turnover per breath for a period of several dive cycles if the appropriate mean and variance of V_T and EO_2 can be modeled. Here, we pursue that logic to estimate the energy turnover per breath in wild humpback whales using a Monte Carlo modeling approach, where random samples from the probability density functions of V_T and EO_2 are multiplied to form a probability density function of $VO_{2\text{breath}}$.

Using a standard body mass of 30 t for an adult humpback whale (18, 55), we estimate the TLC from the equation (56)

$$\text{TLC} = 0.135 \cdot M_b^{0.92} \quad (2)$$

We then estimate the VC (the highest possible V_T) to be a high proportion (85%) of TLC sensu (42, 57–59).

$$\text{VC} = 0.85 \cdot \text{TLC} \quad (3)$$

Drone footage of open nares during breaths in wild humpback whales (60) suggests that V_T , like for any other breathing mammal (61), is variable. To embrace that variation in our modeling, we created a probability density distribution of V_T with a mean of 0.6 of VC sensu (44) and an SD of 150 liters, corresponding to 0.1 of VC, resulting in a 5 to 95% confidence interval for V_T from 0.4 to 0.8 of VC (Fig. 3A). Using a mean of 0.6·VC which is about four times the value for resting terrestrial mammals (62) and two times higher than for smaller, free-moving marine mammals (16) may lead to consistent overestimation of V_T and hence VO_2 per breath in wild humpback whales. However, because we test the hypothesis that lunge feeding is expensive, we deliberately wish to bias toward overestimating lunge costs. Thus, by using a V_T distribution from 0.4 to 0.8 of VC, we ensure that the extreme consequences of even the highest consistent V_T are propagated in the modeling allowing us to put a maximum cap on $VO_{2\text{breath}}$.

The extraction coefficient of the lung (EO_2) can be up to 80% after prolonged breath holds in diving marine mammals (53, 63) but drops to a quarter of that after a number of breaths during a surfacing interval (64). This complicates the estimation of EO_2 for an individual breath in a wild animal, but because the blood pH for any mammal (65) must be stable around 7.4, we can use the lung gas equation to estimate the distribution of average realized EO_2 over longer time periods.

The lung gas equation describes the relationship between alveolar CO_2 and O_2 at a given inspired PO_2 and a respiratory gas

exchange ratio (R). This was first given by (66)

$$P_{AO_2} = P_{IO_2} - \frac{P_A CO_2}{R} + \left[F_{IO_2} \cdot P_A CO_2 \cdot \left(\frac{1-R}{R} \right) \right] \quad (4)$$

where P_{AO_2} and $P_A CO_2$ are the alveolar oxygen and carbon dioxide partial pressures, P_{IO_2} and F_{IO_2} the inspired oxygen partial pressure and fractional concentration, and R is the respiratory exchange ratio. Assuming that CO_2 is in equilibrium across the lung membrane, we can replace $P_A CO_2$ with $P_a CO_2$, and rewriting the original Eq. 4, we get

$$P_{AO_2} = P_{IO_2} - \frac{P_a CO_2}{R} [1 - (1-R)F_{IO_2}] \quad (5)$$

The extraction coefficient EO_2 is defined in terms of the expired oxygen partial pressure, but because of the high tidal volume, the dead space fraction becomes low so we can write

$$EO_2 = \frac{P_{IO_2} - P_{EO_2}}{P_{IO_2}} \approx \frac{P_{IO_2} - P_{AO_2}}{P_{IO_2}} \quad (6)$$

Thus, EO_2 can be estimated if $P_a CO_2$ can be either measured or estimated with reasonable certainty. Direct measurements of $P_a CO_2$ in large free-roaming cetaceans is impossible, but here, we exploit the fact that $P_a CO_2$ on average is unexpectedly stable across both terrestrial mammals and all measured marine mammals [fig. S7; (67)] between 30 and 56 mmHg. Using Eqs. 5 and 6, these $P_a CO_2$ values translate into EO_2 values between 0.24 and 0.45. EO_2 can for any given breath be both higher and lower, but in the steady-state situation where the blood pH is 7.4 and the body temperature is 37°C, the mean EO_2 per breath cannot be higher than 0.35. To estimate $VO_{2\text{breath}}$, we therefore assume a mean EO_2 in our probability density function of 0.35 with 5 and 95% confidence interval of 0.3 and 0.4, consistent with previously measured $P_a CO_2$ values (42, 45, 67, 68) (fig. S7). This use of Eqs. 3, 5, and 6 also shows that previous assumptions (47–50, 69, 70) of average EO_2 of 0.5 are physiologically untenable.

Yearly energy expenditure and prey intake in a lunge

To estimate the yearly prey consumption of free-living humpback whales, we used our measured breathing rates on feeding grounds (median = 1.2 breaths min^{-1}) and previously published breathing rates on breeding grounds (median = 0.7 breaths min^{-1}) (fig. S8) (15). Because, to our knowledge, data on breathing rates of migrating humpback whales are unavailable, we assumed that the value for migrating, but largely fasting individuals would be half way between that on feeding grounds and on breeding grounds (median = 0.95 breaths min^{-1}). This assumption is based on previous observations showing a positive correlation between breathing rate and swim speed in gray whales (*E. robustus*) (69) and minke whales (*Balaenoptera acutorostrata*) (49) in conjunction with calculated faster swim speeds for migrating humpback whales compared to when they are on their breeding grounds (71). We then modeled a distribution of each breathing rate with an SD of 0.2 of the mean (fig. S8).

The time spent on feeding, migrating, and breeding during a year has been shown to vary between humpback whale populations, as well as with sex, maturity, and migration routes (24, 71, 72). Thus, the duration of effective feeding (120 days, SD 15 days), migration (145 days, SD 15 days) and breeding (100 days, SD 15 days) periods during a year was modeled to incorporate this variability. Using the

distributions of breathing rates and total times spent in each activity in a year, we estimated the probability distribution of total number ($N_{\text{breath_year}}$) of breaths in a year (Fig. 3F). We then used this to estimate the total yearly FMR distribution by multiplying random samples from the $N_{\text{breath_year}}$ distribution with random samples from the probability distribution of energetic turnover per breath (Eq. 7).

$$\text{FMR}_{\text{year}} = N_{\text{breath_year}} \cdot \text{VO}_{2\text{breath}} \cdot \epsilon\text{O}_2 \quad (7)$$

Here, ϵO_2 is the energetic value of oxygen, which is 20.08 kJ·liter⁻¹. Daily FMR on the feeding ground was calculated in the same fashion using the total number of breaths in a day, $N_{\text{breath_day}}$ (Fig. 3E).

To convert yearly energy requirements to prey mass, we used the mean energetic value of capelin and krill, two common humpback whale prey types in their feeding areas (35, 73). The prey energetic density of krill varies with species, sex, and time of year (74). For a common Antarctic krill type, *Euphausia superba*, the energetic value has been measured at 3.8 to 5.4 MJ kg⁻¹ ww (9, 74). Similar values were found for krill species in Greenland and Iceland (*Thysanoessa raschii* and *Meganocyttiphanes norvegica*) 3.9 to 6.4 MJ kg⁻¹ ww (75, 76) and for two other species of krill (*Thysanoessa spinifera* and *Euphausia pacifica*) 2.94 to 3.8 MJ kg⁻¹ ww (21). For capelin (*Mallotus villosus*, Osmeridae) in Greenland, the energy density is, on average, 4.2 MJ kg⁻¹ ww (77) but can also vary between sex and season (78). Therefore, to account for a mixed diet, we took the average of these two prey energetic values (11, 79). The ingested prey energy further depends on the digestive assimilation coefficient, which in baleen whales, like for other marine mammals, has been estimated to be ~90% (19). Accounting for the digestive assimilation coefficient, the available energy density per kilo of prey consumed is 3.6 MJ kg⁻¹ (i.e., 4 MJ*0.9). It is important to note that some prey types of humpback whales have a much higher energetic density per kilo [up to 6 to 10 MJ kg⁻¹ (75)] and by targeting these energetic prey a humpback whale would need to ingest less prey mass per lunge and per feeding season (tons) for the same yearly energetic requirement (MJ). If such prey are targeted consistently, we overestimate the prey weights per lunge and yearly-required prey tonnage.

To estimate how much prey a humpback whale needs to ingest on average during a lunge to meet its overall energy costs, we first modeled effective feeding days, i.e., the number of days in which the whale actively feeds while on feeding grounds, with an average of 120 days and an SD of 15 days based on previous observations (11, 80). By dividing random samples from the annual prey requirement distribution in tons by random samples from the modeled distribution of the effective number of feeding days, we can then estimate the distribution of needed daily prey consumption for a pregnant humpback whale on the feeding grounds (6549 ± 1623 MJ, 1.8 ± 0.5 t). To get the required average prey intake per lunge, we divided random samples from the daily prey consumption distribution with random samples from the distribution of number of daily lunges to find that the mean estimated intake per lunge should be around 3.8 kg of mixed prey (13.8 ± 7.4 MJ, 3.8 ± 2 kg) (Fig. 3J). Pregnant female humpback whales will have an increased energy need to fuel the growth of their calf during pregnancy and after birth while lactating. Earlier studies on baleen whales have estimated the cost of gestation and lactation at ~20% of total energy cost over a 2-year period (81, 82), thus, a pregnant female need to

ingest 20% more energy during two subsequent feeding seasons. If we allocate that to extra food consumption during each feeding season then a reproducing female humpback whale needs to ingest 18.8 ± 4.5 t (67,800 ± 16,300 MJ) more prey than a nonreproducing female each feeding season to produce a viable calf every 2 years.

The cost of a lunge

The hourly breathing rates of humpback whales increased with increased lunge rates (Fig. 2). The cost (expressed in number of breaths) of performing a lunge can be estimated on the log-scale from the fitted model parameters [$\log(\text{Breaths}) = 4.1134 + 0.0069 \cdot \text{Lunges}$]. When back transforming the predicted values of the GLMM to the arithmetic scale however, the regression line between the relationship between number of breaths and number of lunges becomes curvilinear because of the log-link being used in the model (Fig. 2). To obtain a mean estimate of the cost per lunge, we therefore calculated the overall increase in number of breaths from 0 to 88 lunges (the full range of lunge values observed) and divided it by the maximum number of lunges (i.e. 88), which is equivalent to the slope of a linear regression line fitted between the number of breaths and number of lunges on the arithmetic scale. The estimated slope was 0.58, which corresponds to a marginal lunge cost of 60% the energetic turnover of an average breath. We found the same slopes if we binned the breath and lunge data over 0.5- or 2-hour epochs.

A lung ventilation corresponds to a median energy turnover of 1.33 ± 0.3 MJ (Fig. 3D). To account for heavier breathing during exercise (16), i.e. a high $\text{VO}_{2\text{breath}}$, we used the 95% percentile of the distribution of energetic turnover per breath (1.76 MJ) when calculating the maximum cost associated with lunging. The maximum energetic cost of a lunge was thereby calculated to be 1.02 MJ (Cost of lunge = 0.58*energetic turnover per breath of 1.76 MJ) and the median cost calculated to be 0.77 MJ (Cost of lunge = 0.58*energetic turnover per breath of 1.33 MJ). If the whales are digesting while foraging, part of these elevated breathing rates with increasing lunge rates will be due to specific dynamic action costs, but we conservatively assume these to be zero thereby, if anything, overestimating lunge costs.

Assuming an assimilation efficiency of 90% (19), and an average calorific value of prey, the median cost of a lunge corresponds to 225 g of prey or a maximum of 298 g using the 95% [using the average value of 3800 kJ kg⁻¹ krill ww (9, 11, 74)]. If we translate the maximum energetic cost of performing a lunge into muscle action, a 30-t humpback whale would perform mechanical work of about 8.3 J kg⁻¹ of body mass per lunge (Eq. 8), assuming a muscle efficiency of 25%. In comparison, the same mass-specific mechanical work would be done by a terrestrial animal climbing ~87 cm vertically (Eq. 9).

$$\text{Mechanical work} \left(\frac{\text{J}}{\text{kg}} \right) = \frac{1 \cdot 10^6 \text{ J}}{30,000 \text{ kg}} \cdot 0.25 \quad (8)$$

$$\text{Potential energy (J)} = \text{mass (kg)} \cdot 9.82 \left(\frac{\text{m}}{\text{s}^2} \right) \cdot \text{height (m)} \quad (9)$$

Supplementary Materials

This PDF file includes:

Supplementary Text
Figs. S1 to S14
Table S1
Legends for audio S1 to S3
Legends for movies S1 to S6
Legend for data S1
References

Other Supplementary Material for this manuscript includes the following:

Audio S1 to S3
Movies S1 to S6
Data S1

REFERENCES AND NOTES

- J. A. Goldbogen, P. T. Madsen, The evolution of foraging capacity and gigantism in cetaceans. *J. Exp. Biol.* **221**, jeb166033 (2018).
- G. J. Slater, J. A. Goldbogen, N. D. Pyenson, Independent evolution of baleen whale gigantism linked to Plio-Pleistocene ocean dynamics. *Proc. R. Soc. B Biol. Sci.* **284**, 20170546 (2017).
- R. E. Shadwick, J. Potvin, J. A. Goldbogen, Lunge feeding in Rorqual Whales. *Physiology* **34**, 409–418 (2019).
- M. Simon, M. Johnson, P. T. Madsen, Keeping momentum with a mouthful of water: Behavior and kinematics of humpback whale lunge feeding. *J. Exp. Biol.* **215**, 3786–3798 (2012).
- D. E. Cade, A. S. Friedlaender, J. Calambokidis, J. A. Goldbogen, Kinematic Diversity in Rorqual Whale Feeding Mechanisms. *Curr. Biol.* **26**, 2617–2624 (2016).
- J. A. Goldbogen, J. Calambokidis, D. A. Croll, M. F. McKenna, E. Oleson, J. Potvin, N. D. Pyenson, G. Schorr, R. E. Shadwick, B. R. Tershy, Scaling of lunge-feeding performance in rorqual whales: Mass-specific energy expenditure increases with body size and progressively limits diving capacity. *Funct. Ecol.* **26**, 216–226 (2012).
- A. Acevedo-Gutiérrez, D. A. Croll, B. R. Tershy, High feeding costs limit dive time in the largest whales. *J. Exp. Biol.* **205**, 1747–1753 (2002).
- J. A. Goldbogen, J. Calambokidis, D. A. Croll, J. T. Harvey, K. M. Newton, E. M. Oleson, G. Schorr, R. E. Shadwick, Foraging behavior of humpback whales: Kinematic and respiratory patterns suggest a high cost for a lunge. *J. Exp. Biol.* **211**, 3712–3719 (2008).
- J. A. Goldbogen, D. E. Cade, D. M. Wisniewska, J. Potvin, P. S. Segre, M. S. Savoca, E. L. Hazen, M. F. Czapanskiy, S. R. Kahane-Rapport, S. L. DeRuiter, S. Gero, P. Tønnesen, W. T. Gough, M. B. Hanson, M. M. Holt, F. H. Jensen, M. Simon, A. K. Stimpert, P. Arranz, D. W. Johnston, D. P. Nowacek, S. E. Parks, F. Visser, A. S. Friedlaender, P. L. Tyack, P. T. Madsen, N. D. Pyenson, Why whales are big but not bigger: Physiological drivers and ecological limits in the age of ocean giants. *Science* **366**, 1367–1372 (2019).
- M. F. Czapanskiy, M. S. Savoca, W. T. Gough, P. S. Segre, D. M. Wisniewska, D. E. Cade, J. A. Goldbogen, Modelling short-term energetic costs of sonar disturbance to cetaceans using high-resolution foraging data. *J. Appl. Ecol.* **58**, 1643–1657 (2021).
- M. S. Savoca, M. F. Czapanskiy, S. R. Kahane-Rapport, W. T. Gough, J. A. Fahlbusch, K. C. Bierlich, P. S. Segre, J. Di Clemente, G. S. Penry, D. N. Wiley, J. Calambokidis, D. P. Nowacek, D. W. Johnston, N. D. Pyenson, A. S. Friedlaender, E. L. Hazen, J. A. Goldbogen, Baleen whale prey consumption based on high-resolution foraging measurements. *Nature* **599**, 85–90 (2021).
- C. Lockyer, Growth and energy budgets of large baleen whales from the Southern Hemisphere, in *Mammals in the Seas*, J. G. Clark, Ed. (FAO Fish. Ser. no. 5, 1981) vol. 3, pp. 379–487.
- L. Ratnarajah, A. R. Bowie, D. Lannuzel, K. M. Meiners, S. Nicol, The biogeochemical role of baleen whales and krill in Southern Ocean nutrient cycling. *PLOS ONE* **9**, e114067 (2014).
- J. Roman, J. J. McCarthy, The Whale Pump: Marine Mammals Enhance Primary Productivity in a Coastal Basin. *PLOS ONE* **5**, e13255 (2010).
- L. Bejder, S. Videsen, L. Hermanssen, M. Simon, D. Hanf, P. T. Madsen, Low energy expenditure and resting behaviour of humpback whale mother-calf pairs highlights conservation importance of sheltered breeding areas. *Sci. Rep.* **9**, 771 (2019).
- A. Fahlman, J. van der Hoop, M. J. Moore, G. Levine, J. Rocho-Levine, M. Brodsky, Estimating energetics in cetaceans from respiratory frequency: Why we need to understand physiology. *Biol. Open* **5**, 436–442 (2016).
- N. C. Heglund, M. A. Fedak, C. R. Taylor, G. A. Cavagna, Energetics and mechanics of terrestrial locomotion. IV. Total mechanical energy changes as a function of speed and body size in birds and mammals. *J. Exp. Biol.* **97**, 57–66 (1982).
- P. S. Segre, J. Potvin, D. E. Cade, J. Calambokidis, J. Di Clemente, F. E. Fish, A. S. Friedlaender, W. T. Gough, S. R. Kahane-Rapport, C. Oliveira, S. E. Parks, G. S. Penry, M. Simon, A. K. Stimpert, D. N. Wiley, K. C. Bierlich, P. T. Madsen, J. A. Goldbogen, Energetic and physical limitations on the breaching performance of large whales. *eLife* **9**, e51760 (2020).
- P.-E. Mårtensson, E. S. Nordøy, A. S. Blix, Digestibility of krill (*Euphausia superba* and *Thysanoessa* sp.) in minke whales (*Balaenoptera acutorostrata*) and crabeater seals (*Lobodon carcinophagus*). *Br. J. Nutr.* **72**, 713–716 (1994).
- W. T. Gough, D. E. Cade, M. F. Czapanskiy, J. Potvin, F. E. Fish, S. R. Kahane-Rapport, M. S. Savoca, K. C. Bierlich, D. W. Johnston, A. S. Friedlaender, A. Szabo, L. Bejder, J. A. Goldbogen, Fast and Furious: Energetic Tradeoffs and Scaling of High-Speed Foraging in Rorqual Whales. *Integr. Org. Biol.* **4**, obac038 (2022).
- E. M. Chenoweth, K. M. Boswell, A. S. Friedlaender, M. V. McPhee, J. A. Burrows, R. A. Heintz, J. M. Straley, Confronting assumptions about prey selection by lunge-feeding whales using a process-based model. *Funct. Ecol.* **35**, 1722–1734 (2021).
- D. E. Cade, N. Carey, P. Domenici, J. Potvin, J. A. Goldbogen, Predator-informed looming stimulus experiments reveal how large filter feeding whales capture highly maneuverable forage fish. *Proc. Natl. Acad. Sci. U.S.A.* **117**, 472–478 (2020).
- F. Christiansen, A. M. Dujon, K. R. Sprogis, J. P. Y. Arnould, L. Bejder, Noninvasive unmanned aerial vehicle provides estimates of the energetic cost of reproduction in humpback whales. *Ecosphere* **7**, e01468 (2016).
- W. H. Dawbin, The seasonal migratory cycle of humpback whales. *Univ. Calif. Press*, 145–170 (1966).
- T. M. Williams, M. Peter-Heide Jørgensen, A. M. Pagano, C. M. Bryce, Hunters versus hunted: New perspectives on the energetic costs of survival at the top of the food chain. *Funct. Ecol.* **34**, 2015–2029 (2020).
- M. Diaz Gomez, D. A. S. Rosen, A. W. Trites, Net energy gained by northern fur seals (*Callorhinus ursinus*) is impacted more by diet quality than by diet diversity. *Can. J. Zool.* **94**, 123–135 (2016).
- S. R. Kahane-Rapport, J. A. Goldbogen, Allometric scaling of morphology and engulfment capacity in rorqual whales. *J. Morphol.* **279**, 1256–1268 (2018).
- D. P. Nowacek, A. S. Friedlaender, P. N. Halpin, E. L. Hazen, D. W. Johnston, A. J. Read, B. Espinasse, M. Zhou, Y. Zhu, Super-aggregations of krill and humpback whales in Wilhelmina Bay, Antarctic Peninsula. *PLOS ONE* **6**, e19173 (2011).
- D. E. Cade, S. M. Seakamela, K. P. Findlay, J. Fukunaga, S. R. Kahane-Rapport, J. D. Warren, J. Calambokidis, J. A. Fahlbusch, A. S. Friedlaender, E. L. Hazen, D. Kotze, S. McCue, M. Mejer, W. K. Oestreich, M. G. Oudejans, C. Wilke, J. A. Goldbogen, Predator-scale spatial analysis of intra-patch prey distribution reveals the energetic drivers of rorqual whale super-group formation. *Funct. Ecol.* **35**, 894–908 (2021).
- M. Bejder, D. W. Johnston, J. Smith, A. S. Friedlaender, L. Bejder, Embracing conservation success of recovering humpback whale populations: Evaluating the case for downlisting their conservation status in Australia. *Mar. Policy* **66**, 137–141 (2016).
- P. Stevick, J. Allen, P. Clapham, N. Friday, S. Katona, F. Larsen, J. Lien, D. Mattila, P. Palsboll, J. Sigurjónsson, T. Smith, N. Øien, P. Hammond, North Atlantic humpback whale abundance and rate of increase four decades after protection from whaling. *Mar. Ecol. Prog. Ser.* **258**, 263–273 (2003).
- A. S. Friedlaender, R. B. Tyson, A. K. Stimpert, A. J. Read, D. P. Nowacek, Extreme diel variation in the feeding behavior of humpback whales along the western Antarctic Peninsula during autumn. *Mar. Ecol. Prog. Ser.* **494**, 281–289 (2013).
- S. K. A. Videsen, M. Simon, M. Johnson, P. T. Madsen, F. Christiansen, Cryptic vocal behavior of foraging humpback whales on feeding grounds in West Greenland. *J. Acoust. Soc. Am.* **150**, 2879–2887 (2021).
- L. M. M. López, P. J. O. Miller, N. Aguilar de Soto, M. Johnson, Gait switches in deep-diving beaked whales: Biomechanical strategies for long-duration dives. *J. Exp. Biol.* **218**, 1325–1338 (2015).
- D. E. Cade, S. R. Kahane-Rapport, B. Wallis, J. A. Goldbogen, A. S. Friedlaender, Evidence for size-selective predation by Antarctic humpback whales. *Front. Mar. Sci.* **9**, 747788 (2022).
- P. J. O. Miller, A. D. Shapiro, V. B. Deecke, The diving behaviour of mammal-eating killer whales (*Orcinus orca*): Variations with ecological not physiological factors. *Can. J. Zool.* **88**, 1103–1112 (2010).
- S. Isojunno, D. Sadykova, S. DeRuiter, C. Curé, F. Visser, L. Thomas, P. J. O. Miller, C. M. Harris, Individual, ecological, and anthropogenic influences on activity budgets of long-finned pilot whales. *Ecosphere* **8**, e02044 (2017).
- W. F. Dolphin, Ventilation and dive patterns of humpback whales, *Megaptera novaeangliae*, on their Alaskan feeding grounds. *Can. J. Zool.* **65**, 83–90 (1987).
- A. F. Zuur, E. N. Ieno, N. Walker, A. A. Saveliev, G. M. Smith, *Mixed Effects models and Extensions in Ecology with R* (Statistics for Biology and Health, Springer New York, 2009).
- W. N. Venables, B. D. Ripley, *Modern Applied Statistics with S* (Statistics and Computing, Springer New York, 2002).

41. T. M. Williams, T. L. Kendall, B. P. Richter, C. R. Ribeiro-French, J. S. John, K. L. Odell, B. A. Losch, D. A. Feuerbach, M. A. Stamper, Swimming and diving energetics in dolphins: A stroke-by-stroke analysis for predicting the cost of flight responses in wild odontocetes. *J. Exp. Biol.* **220**, 1135–1145 (2017).
42. A. Fahlman, S. H. Loring, G. Levine, J. Rocho-Levine, T. Austin, M. Brodsky, Lung mechanics and pulmonary function testing in cetaceans. *J. Exp. Biol.* **218**, 2030–2038 (2015).
43. A. Fahlman, M. J. Moore, D. Garcia-Parraga, Respiratory function and mechanics in pinnipeds and cetaceans. *J. Exp. Biol.* **220**, 1761–1773 (2017).
44. E. A. Wahrenbrock, G. F. Maruschak, R. Elsner, D. W. Kenney, Respiration and metabolism in two baleen whale calves. *Mar. Fish. Rev.* **36**, 3–8 (1974).
45. J. L. Sumich, Direct and indirect measures of oxygen extraction, tidal lung volumes and respiratory rates in a rehabilitating gray whale calf. *Aquat. Mamm.* **27**, 279–283 (2001).
46. A. Krogh, Physiology of the Blue Whale. *Nature* **133**, 635–637 (1934).
47. A. J. Armstrong, W. R. Siegfried, Consumption of antarctic krill by minke whales. *Antarct. Sci.* **3**, 13–18 (1991).
48. A. S. Blix, L. P. Folkow, Daily energy expenditure in free living minke whales. *Acta Physiol. Scand.* **153**, 61–66 (1995).
49. F. Christiansen, M. H. Rasmussen, D. Lusseau, Inferring energy expenditure from respiration rates in minke whales to measure the effects of whale watching boat interactions. *J. Exp. Mar. Biol. Ecol.* **459**, 96–104 (2014).
50. W. F. Dolphin, Dive behavior and estimated energy expenditure of foraging humpback whales in southeast Alaska. *Can. J. Zool.* **65**, 354–362 (1987).
51. P. F. Scholander, Experimental investigations on the respiratory function in diving mammals and birds. *Hvalrådets Skrifter* **22**, 1–131 (1940).
52. L. Rojano-Doñate, B. I. McDonald, D. M. Wisniewska, M. Johnson, J. Teilmann, M. Wahlberg, J. Hojer-Kristensen, P. T. Madsen, High field metabolic rates of wild harbour porpoises. *J. Exp. Biol.* **221**, jeb185827 (2018).
53. S. H. Ridgway, B. L. Scronce, J. Kanwisher, Respiration and deep diving in the bottlenose porpoise. *Science* **166**, 1651–1654 (1969).
54. J. Z. Reed, C. Chambers, C. J. Hunter, C. Lockyer, R. Kastelein, M. A. Fedak, R. G. Boutilier, Gas exchange and heart rate in the harbour porpoise, *Phocoena phocoena*. *J. Comp. Physiol. B.* **170**, 1–10 (2000).
55. C. Lockyer, Body weights of some species of large whales. *ICES J. Mar. Sci.* **36**, 259–273 (1976).
56. G. L. Kooyman, E. E. Sinnett, Mechanical properties of the harbor porpoise lung, *Phocoena phocoena*. *Respir. Physiol.* **36**, 287–300 (1979).
57. G. L. Kooyman, Respiratory adaptations in marine mammals. *Am. Zool.* **13**, 457–468 (1973).
58. G. L. Kooyman, M. A. Castellini, R. W. Davis, Physiology of diving in marine mammals. *Annu. Rev. Physiol.* **43**, 343–356 (1981).
59. C. R. Olsen, F. C. Hale, R. Elsner, Mechanics of ventilation in the pilot whale. *Respir. Physiol.* **7**, 137–149 (1969).
60. M. C. I. Martins, C. Miller, P. Hamilton, J. Robbins, D. P. Zitterbart, M. Moore, Respiration cycle duration and seawater flux through open blowholes of humpback (*Megaptera novaeangliae*) and North Atlantic right (*Eubalaena glacialis*) whales. *Mar. Mamm. Sci.* **36**, 1160–1179 (2020).
61. D. M. Bramble, D. R. Carrier, Running and breathing in mammals. *Science* **219**, 251–256 (1983).
62. W. R. Stahl, Scaling of respiratory variables in mammals. *J. Appl. Physiol.* **22**, 453–460 (1967).
63. P. J. Ponganis, G. L. Kooyman, M. A. Castellini, Determinants of the aerobic dive limit of Weddell seals: Analysis of diving metabolic rates, postdive end tidal PO_2s , and blood and muscle oxygen stores. *Physiol. Zool.* **66**, 732–749 (1993).
64. A. Fahlman, M. Brodsky, S. Miedler, S. Dennison, M. Ivančić, G. Levine, J. Rocho-Levine, M. Manley, J. Rocabert, A. Borque Espinosa, Ventilation and gas exchange before and after voluntary static surface breath-holds in clinically healthy bottlenose dolphins, *Tursiops truncatus*. *J. Exp. Biol.* **222**, jeb192211 (2019).
65. N. K. Iversen, H. Malte, E. Baatrup, T. Wang, The normal acid–base status of mice. *Respir. Physiol. Neurobiol.* **180**, 252–257 (2012).
66. W. O. Fenn, H. Rahn, A. B. Otis, A theoretical study of the composition of the alveolar air at altitude. *Am. J. Physiol.* **146**, 637–653 (1946).
67. J. P. Mortola, J. Seguin, End-tidal CO_2 in some aquatic mammals of large size. *Zoology (Jena)* **112**, 77–85 (2009).
68. J. L. Sumich, Oxygen extraction in free-swimming gray whale calves. *Mar. Mamm. Sci.* **10**, 226–230 (1994).
69. J. L. Sumich, Swimming velocities, breathing patterns, and estimated costs of locomotion in migrating gray whales, *Eschrichtius robustus*. *Can. J. Zool.* **61**, 647–652 (1983).
70. L. P. Folkow, A. S. Blix, Metabolic rates of minke whales (*Balaenoptera acutorostrata*) in cold water. *Acta Physiol. Scand.* **146**, 141–150 (1992).
71. A. S. Kennedy, A. N. Zerbini, O. V. Vásquez, N. Gandilhon, P. J. Clapham, O. Adam, Local and migratory movements of humpback whales Atlantic Ocean. *NRC Res. Press.* **18**, 9–18 (2014).
72. R. G. Chittleborough, Dynamics of two populations of the humpback whale, *Megaptera novaeangliae* (Borowski). *Mar. Freshw. Res.* **16**, 33–128 (1965).
73. A. A. Cabrera, E. Schall, M. Bérubé, P. Anderwald, L. Bachmann, S. Berrow, P. B. Best, P. J. Clapham, H. A. Cunha, L. Dalla Rosa, C. Dias, K. P. Findlay, T. Haug, M. P. Heide-Jørgensen, A. R. Hoelzel, K. M. Kovacs, S. Landry, F. Larsen, X. M. Lopes, C. Lydersen, D. K. Mattila, T. Oosting, R. M. Pace, C. Papetti, A. Paspati, L. A. Pastene, R. Prieto, C. Ramp, J. Robbins, R. Sears, E. R. Secchi, M. A. Silva, M. Simon, G. Víkingsson, Ø. Wiig, N. Øien, P. J. Palsbøll, Strong and lasting impacts of past global warming on baleen whales and their prey. *Glob. Chang. Biol.* **28**, 2657–2677 (2022).
74. A. Clarke, The biochemical composition of krill, *Euphausia superba* Dana, from South Georgia. *J. Exp. Mar. Biol. Ecol.* **43**, 221–236 (1980).
75. F. R. Merkel, J. F. Linnebjerg, O. G. N. Andersen, N. P. Huffeldt, T. Jansen, R. Hedeholm, M. Frederiksen, Changing winter diet of thick-billed murres (*Uria lomvia*) in southwest Greenland, 1990s versus 2010s. *Can. J. Zool.* **99**, 1080–1088 (2021).
76. C. Lockyer, in *Approaches to Marine Mammal Energetics*, A. C. Huntley, D. P. Costa, G. A. J. Worthy, M. A. C. Huntley, Eds. (Society for Marine Mammalogy, 1987), pp. 183–203.
77. R. Hedeholm, P. Grønkvær, S. Rysgaard, Energy content and fecundity of capelin (*Mallotus villosus*) along a 1,500-km latitudinal gradient. *Mar. Biol.* **158**, 1319–1330 (2011).
78. W. A. Montevecchi, J. Piatt, Composition and energy contents of mature inshore spawning capelin (*Mallotus villosus*): Implications for seabird predators. *Comp. Biochem. Physiol. Part A Physiol.* **78**, 15–20 (1984).
79. D. Pauly, A. W. Trites, E. Capuli, V. Christensen, Diet composition and trophic levels of marine mammals. *ICES J. Mar. Sci.* **55**, 467–481 (1998).
80. C. S. Baker, L. M. Herman, A. Perry, W. S. Lawton, J. M. Straley, J. H. Straley, Population characteristics and migration of summer and late-season humpback whales (*Megaptera novaeangliae*) in southeastern Alaska. *Mar. Mamm. Sci.* **1**, 304–323 (1985).
81. S. Villegas-Amtmann, L. K. Schwarz, J. L. Sumich, D. P. Costa, D. P. C. Peters, A bioenergetics model to evaluate demographic consequences of disturbance in marine mammals applied to gray whales. *Ecosphere* **6**, 1–19 (2015).
82. C. Lockyer, Review of baleen whale reproduction and implications for management. *Rep. Int. Whal. Comm.* **6**, 27–50 (1984).
83. J. A. Goldbogen, N. D. Pyenson, R. E. Shadwick, Big gulps require high drag for fin whale lunge feeding. *Mar. Ecol. Prog. Ser.* **349**, 289–301 (2007).
84. J. Potvin, D. E. Cade, A. J. Werth, R. E. Shadwick, J. A. Goldbogen, Rorqual Lunge-Feeding Energetics Near and Away from the Kinematic Threshold of Optimal Efficiency. *Integr. Org. Biol.* **3**, obab005 (2021).
85. S. R. Kahane-Rapport, M. S. Savoca, D. E. Cade, P. S. Segre, K. C. Bierlich, J. Calambokidis, J. Dale, J. A. Fahlbusch, A. S. Friedlaender, D. W. Johnston, A. J. Werth, J. A. Goldbogen, Lunge filter feeding biomechanics constrain rorqual foraging ecology across scale. *J. Exp. Biol.* **223**, jeb224196 (2020).
86. J. A. Goldbogen, J. Potvin, R. E. Shadwick, Skull and buccal cavity allometry increase mass-specific engulfment capacity in fin whales. *Proc. R. Soc. B Biol. Sci.* **277**, 861–868 (2010).
87. W. T. Gough, P. S. Segre, K. C. Bierlich, D. E. Cade, J. Potvin, F. E. Fish, J. Dale, J. Di Clemente, A. S. Friedlaender, D. W. Johnston, S. R. Kahane-Rapport, J. Kennedy, J. H. Long, M. Oudejans, G. Penry, M. S. Savoca, M. Simon, S. K. A. Videse, F. Visser, D. N. Wiley, J. A. Goldbogen, Scaling of swimming performance in baleen whales. *J. Exp. Biol.* **222**, jeb204172 (2019).
88. J. Potvin, J. A. Goldbogen, R. E. Shadwick, Metabolic expenditures of lunge feeding rorquals Across scale: Implications for the evolution of filter feeding and the limits to maximum body size. *PLOS ONE* **7**, e44854 (2012).
89. D. E. Cade, S. M. Seakamela, K. P. Findlay, J. Fukunaga, S. R. Kahane-Rapport, J. D. Warren, J. Calambokidis, J. A. Fahlbusch, A. S. Friedlaender, E. L. Hazen, D. Kotze, S. McCue, M. Mejer, W. K. Oestreich, M. G. Oudejans, C. Wilke, J. A. Goldbogen, Super-group data archive. Stanford Digital Repository (2021); <https://purl.stanford.edu/rq794kc6747>.
90. C. Lockyer, T. Waters, Weights and anatomical measurements of northeastern Atlantic fin (*Balaenoptera physalus*, Linnaeus) and Sei (*B. borealis*, Lesson) whales. *Mar. Mamm. Sci.* **2**, 169–185 (1986).
91. G. L. Kooyman, D. H. Kerem, W. B. Campbell, J. J. Wright, Pulmonary gas exchange in freely diving Weddell seals *Leptonychotes weddellii*. *Respir. Physiol.* **17**, 283–290 (1973).
92. A. Fahlman, M. Brodsky, R. Wells, K. McHugh, J. Allen, A. Barleycorn, J. C. Sweeney, D. Fauquier, M. Moore, Field energetics and lung function in wild bottlenose dolphins, *Tursiops truncatus*, in Sarasota bay Florida. *R. Soc. Open Sci.* **5**, 171280 (2018).
93. A. Fahlman, J. Meegan, A. Borque-Espinosa, E. D. Jensen, Pulmonary function and resting metabolic rates in California sea lions (*Zalophus californianus*) on land and in water. *Aquat. Mamm.* **46**, 67–79 (2020).

94. A. Fahlman, J. Madigan, Respiratory function in voluntary participating patagonia sea lions (*Otaria flavescens*) in sternal recumbency. *Front. Physiol.* **7**, 528 (2016).
95. J. Z. Reed, C. Chambers, M. A. Fedak, P. J. Butler, Gas exchange of captive freely diving grey seals (*Halichoerus grypus*). *J. Exp. Biol.* **191**, 1–18 (1994).
96. M. Allen, D. Poggiali, K. Whitaker, T. R. Marshall, R. A. Kievit, Raincloud plots: A multi-platform tool for robust data visualization. *Wellcome Open Res.* **4**, 63 (2019).
97. M. Kleiber, Metabolic turnover rate: A physiological meaning of the metabolic rate per unit body weight. *J. Theor. Biol.* **53**, 199–204 (1975).
98. K. A. Nagy, Field metabolic rate and body size. *J. Exp. Biol.* **208**, 1621–1625 (2005).

Acknowledgments: For fieldwork in Antarctica, we thank D. Nowacek, A. Stimpert, and R. Tyson. For fieldwork in Greenland, we thank the crew of R/V Sanna, A. Brandt, A. Isaksen, T. Boye, F. Ugarte, B. K. Nielsen, M. Møller, K. Tubbert, L. Heilman, M. Ladegaard, T. Hurst, P. Hegelund, and S. Perez. **Funding:** This work is supported by the Aage V. Jensen Foundation (S.K.A.V. and M.S.), Independent Research Fund Denmark | Natural Sciences (P.T.M.), the National Science Foundation (A.F.), Office of Polar Programs Grant ANT-07-39483 (A.F.); Danish Ministry of Higher

Education and Science (M.S.); the Aarhus University Research Foundation (M.J.); EU H2020 research and innovation program under Marie Skłodowska-Curie grant 754513 (M.J.); the Carlsberg Foundation (M.S.); and Greenland Climate Research Centre, Danish Ministry of Higher Education and Science (M.S.). **Author contributions:** Conceptualization: S.K.A.V. and P.T.M. Methodology: S.K.A.V., P.T.M., H.M., T.W., and M.J. Investigation: P.T.M., M.J., M.S., A.F., S.K.A.V., P.S., and J.G. Data curation: S.K.A.V. Formal analysis: S.K.A.V. and F.C. Visualization: S.K.A.V. and P.T.M. Supervision: P.T.M. Writing—original draft: S.K.A.V., M.J., and P.T.M. Writing—review and editing: S.K.A.V., M.J., P.T.M., F.C., H.M., A.F., J.G., M.S., P.S., and T.W. **Competing interests:** The authors declare that they have no competing interests. **Data and materials availability:** All data needed to evaluate the conclusions in the article are present in the paper and in the Supplementary Materials.

Submitted 12 August 2022

Accepted 22 May 2023

Published 23 June 2023

10.1126/sciadv.ade3889